

Published in final edited form as:

J Am Chem Soc. 2007 November 7; 129(44): 13537–13543. doi:10.1021/ja073724k.

Free Energy Perturbation (FEP) Simulation on the Transition-States of Cocaine Hydrolysis Catalyzed by Human Butyrylcholinesterase and Its Mutants

Yongmei Pan, Daquan Gao, Wenchao Yang, Hoon Cho^a, and Chang-Guo Zhan^{*}

Department of Pharmaceutical Sciences, College of Pharmacy, University of Kentucky, 725 Rose Street, Lexington, KY 40536

Abstract

A novel computational protocol based on free energy perturbation (FEP) simulations on both the free enzyme and transition state structures has been developed and tested to predict the mutation-caused shift of the free energy change from the free enzyme to the rate-determining transition state for human butyrylcholinesterase (BChE)-catalyzed hydrolysis of (-)-cocaine. The calculated shift, denoted by $\Delta\Delta G(1\rightarrow 2)$, of such kind of free energy change determines the catalytic efficiency (k_{cat}/K_M) change caused by the simulated mutation transforming enzyme 1 to enzyme 2. By using the FEP-based computational protocol, the $\Delta\Delta G(1\rightarrow 2)$ values for the mutations A328W/Y332A \rightarrow A328W/Y332G and A328W/Y332G \rightarrow A328W/Y332G/A199S were calculated to be -0.22 and -1.94 kcal/mol, respectively. The calculated $\Delta\Delta G(1\rightarrow 2)$ values predict that the change from the A328W/Y332A mutant to the A328W/Y332G mutant should slightly improve the catalytic efficiency and that the change from the A328W/Y332G mutant to the A328W/Y332G/A199S mutant should significantly improve the catalytic efficiency of the enzyme for the (-)-cocaine hydrolysis. The predicted catalytic efficiency increases are supported by the experimental data showing that $k_{\text{cat}}/K_M = 8.5 \times 10^6$, 1.4×10^7 , and $7.2 \times 10^7 \text{ min}^{-1} \text{ M}^{-1}$ for the A328W/Y332A, A328W/Y332G, and A328W/Y332G/A199S mutants, respectively. The qualitative agreement between the computational and experimental data suggests that the FEP simulations may provide a promising protocol for rational design of high-activity mutants of an enzyme. The general computational strategy of the FEP simulation on a transition state can be used to study the effects of a mutation on the activation free energy for any enzymatic reaction.

Introduction

Cocaine is well known for its high potential of addiction and the significant consequences of its abuse.¹⁻³ The disastrous medical and social consequences of cocaine addiction have made the development of an effective pharmacological treatment a high priority.⁴⁻⁶ It is commonly believed that cocaine mediates its reinforcing and toxic effects by blocking neurotransmitter reuptake in the central nervous system (CNS). However, the classical pharmacodynamic approach, which means to design small molecules to target the related transporters or receptors in CNS, has failed to yield a really useful antagonist due to the difficulties inherent in blocking

^{*} To whom correspondence should be addressed.: Chang-Guo Zhan, Ph.D., Associate Professor, Department of Pharmaceutical Sciences, College of Pharmacy, University of Kentucky, 725 Rose Street, Lexington, KY 40536, TEL: 859-323-3943, FAX: 859-323-3575, zhan@uky.edu.

^aPresent address: College of Engineering, Chosun University, Gwangju 501-759, South Korea

Supporting Information Available. Complete citations of references 34 and 35, detailed information about the FEP results and parameters developed *etc.*, and the experimental methods. This material is available free of charge *via* the Internet at <http://pubs.acs.org>.

a blocker.^{1-4,6} An alternative approach is to interfere with the delivery of cocaine to its receptors or accelerate its metabolism in the body.^{4,7-17} Butyrylcholinesterase (BChE), the principal plasma enzyme that catalyzes cocaine hydrolysis into its biologically inactive metabolites, is an ideal target for this purpose. There are some clear advantages of using this enzyme to accelerate the cocaine metabolism.^{4,18} First, the metabolites of cocaine catalyzed by this enzyme are all biologically inactive and, therefore, the metabolites produced in this pathway have no toxic effects as cocaine.¹⁹ Second, human BChE has a long history of clinic use, and no adverse effect has been noted. Finally, about 20 different naturally occurring mutants of human BChE have been identified, and there is no evidence that these mutants are antigenic.²⁰ However, the catalytic activity of the native form of this plasma enzyme against naturally occurring (-)-cocaine is low. For example, the plasma half-life time of (-)-cocaine is ~45-90 min, long enough for cocaine crossing the blood-brain barrier (BBB) to reach central nervous system (CNS) to make its reinforcing effects.^{21,22} Some mutants of human BChE reported in literature have an improved catalytic efficiency (k_{cat}/K_M) against (-)-cocaine.^{23, 24,25,26} It is still highly desirable for development of a more efficient anti-cocaine medication to design and discover BChE mutants with a significantly improved catalytic efficiency against (-)-cocaine. A high-activity mutant of human BChE is expected to serve as an exogenous enzyme for injection so as to accelerate (-)-cocaine hydrolysis before (-)-cocaine crossing BBB to reach CNS.

Generally speaking, for rational design of a mutant enzyme with a higher catalytic activity for a given substrate, one needs to design a mutation that can accelerate the rate-determining step of the entire catalytic reaction process while the other steps are not slowed down by the mutation. Reported computational modeling and experimental data indicated that the formation of the preactive BChE-(-)-cocaine complex (ES) is the rate-determining step of (-)-cocaine hydrolysis catalyzed by wild-type BChE. Further computational modeling also suggests that the formation of the preactive BChE-(-)-cocaine complex (ES) is hindered mainly by the bulky side chain of Y332 residue in wild-type BChE, but the hindering can be removed by the Y332A or Y332G mutation.²⁴ Therefore, starting from the A328W/Y332A²³ or A328W/Y332G²⁴ mutant, the rational design of further mutation(s) to improve the catalytic efficiency of BChE against (-)-cocaine can aim to decrease the free energy barrier for the first reaction step without significantly affecting the ES formation and other chemical reaction steps. The analysis of previous experimental and computational data available in literature^{19,23,27} clearly shows that the rate-determining step of (-)-cocaine hydrolysis catalyzed by the A328W/Y332A mutant is the first step of the chemical reaction process. Thus, the modeling of the transitional state of this first reaction step (TS1, see Scheme 1) is important for rational design of high-activity mutants of BChE. Furthermore, our recently reported MD simulations show that the hydrogen bonding between the carbonyl oxygen of (-)-cocaine benzoyl ester and the oxyanion hole in the TS1 structure is a crucial factor affecting the transition-state stabilization and the catalytic activity.^{25,26,28,29} Our reported design of BChE mutants have been based on the qualitative understanding of the catalytic mechanism and the TS1 structure. The mutants were designed to enhance the hydrogen bonding between the carbonyl oxygen of (-)-cocaine benzoyl ester and the oxyanion hole of BChE in the TS1 structure,^{25,26} without a quantitative evaluation of the shift (corresponding to a mutation) of the free energy barrier associated with TS1.

In the present study, we aimed to develop a new, efficient computational design strategy and protocol which can be used to theoretically evaluate the shift of the catalytic efficiency from one BChE mutant to another. Our protocol is based on an extension of the well-known free energy perturbation (FEP) approach³⁰ which, in principle, can only be used to simulate the change of a stable structure associated with local minima on the potential energy surface. By using an appropriate computational strategy, we were able to simulate the mutations of both the stable structure of the free enzyme and the rate-determining transition state structure by using the FEP procedure. The FEP simulations on the mutations of both the free enzyme and

transition state allow us to calculate the mutation-caused shift of the free energy change from the free enzyme (BChE) to the rate-determining transition state (*i.e.* TS1)²⁶ and, therefore, to theoretically evaluate/estimate the mutation-caused shift of the catalytic efficiency ($k_{\text{cat}}/K_{\text{M}}$). For validation, the computational protocol has been employed to examine the perturbations corresponding to the mutations A328W/Y332A \rightarrow A328W/Y332G \rightarrow A328W/Y332G/A199S. The computational predictions are consistent with the kinetic data obtained from the wet experiments, suggesting that the FEP-based computational strategy and protocol are valuable for rational design of high-activity mutants of an enzyme.

Computational methods

General consideration of the transition-state simulation

The computational protocol used in the present study is based on the combined use of molecular dynamics (MD) simulation and free energy perturbation (FEP). A critical issue^{25-28,31} should be addressed before describing how we performed any MD or FEP simulation on a transition state structure. In principle, the standard MD and FEP simulation approaches using a classical force field (molecular mechanics) can only simulate a stable structure corresponding to a local minimum on the potential energy surface, whereas a transition state during a reaction process is always associated with a first-order saddle point on the potential energy surface. Hence, MD or FEP simulation using a classical force field cannot directly simulate a transition state without any restraint on the geometry of the transition state. Nevertheless, if we can technically remove the freedom of imaginary vibration in the transition state structure, then the number of vibrational freedoms (normal vibration modes) for a nonlinear molecule will decrease from $3N - 6$. The transition state structure is associated with a local minimum on the potential energy surface within a subspace of the reduced vibrational freedoms, although it is associated with a first-order saddle point on the potential energy surface with all of the $3N - 6$ vibrational freedoms. Theoretically, the vibrational freedom associated with the imaginary vibrational frequency in the transition state structure can be removed by appropriately freezing the reaction coordinate. The reaction coordinate corresponding to the imaginary vibration of the transition state is generally characterized by a combination of some key geometric parameters. Thus, we just need to maintain the bond lengths of the forming and breaking covalent bonds during the MD or FEP simulation on a transition state. Technically, we can maintain the bond lengths of the forming and breaking covalent bonds by simply fixing all atoms within the reaction center, by using some constraints on the forming and breaking covalent bonds, or by redefining the forming and breaking covalent bonds.³¹ The forming and breaking covalent bonds in the transition state will be called “transition” bonds below, for convenience. It should be pointed out that the only purpose of performing such type of MD or FEP simulation on a transition state is to examine the dynamic change of the protein environment surrounding the reaction center and the interaction between the reaction center and the protein environment. Specifically for the transition state structure TS1 depicted in Scheme 1, the reaction coordinate is mainly related to the transition bonds formed within the catalytic triad (including Ser198, Glu325, and His438) and the transition bond between the hydroxyl oxygen of Ser198 side chain and a carbonyl carbon of the cocaine.

For predicting the mutation-caused shifts of the free energies for both the free enzyme and the corresponding TS1 structure, we first performed MD simulations on the unperturbed systems in order to obtain the dynamically stable initial structures required for performing the FEP simulations. Below, we will briefly describe how we carried out the MD and FEP simulations on the free enzyme and TS1 structure.

MD simulation

The initial structures of both the free enzyme and transition state TS1 used in MD simulations were prepared based on our previous MD simulations on wild-type BChE and its mutants A328W/Y332A and A328W/Y332G,²⁴ that were derived from the X-ray crystal structure³² deposited in the Protein Data Bank³³ with pdb code 1POP. The lengths of the transition bonds in the TS1 structure were constrained as those obtained from our previous *ab initio* reaction coordinate calculations on the cocaine hydrolysis catalyzed by wild-type BChE.¹⁹ The partial charges of the cocaine atoms were calculated by using the restrained electrostatic potential-fitting (RESP) protocol implemented in the Antechamber module of Amber7,³⁴ following the electrostatic potential (ESP) calculation at *ab initio* HF/6-31G* level using Gaussian 03 program.³⁵ The geometries used in the ESP calculations came from those obtained from previous *ab initio* reaction coordinate calculations.¹⁹ The charges of the atoms of the oxyanion hole and catalytic triad remain the same with those available in Amber7 package.

All of the MD simulations were performed by using the Sander module of Amber7 package with the same procedures as used in our previous computational studies.²⁴⁻²⁹ For free enzyme structures, the +1 charge of the enzyme was neutralized by adding one chloride counterion. For TS1 structure, the +2 charge of the system was neutralized by adding two chloride counterions. Both the free enzyme and TS1 structures were solvated in a rectangular box of TIP3P water molecule³⁶ with a solute-wall distance of 10 Å. The solvated systems were carefully equilibrated and fully energy-minimized. These systems were gradually heated from $T = 10$ K to $T = 298.15$ K in 40 ps before running the MD simulation at $T = 298.15$ K for 1 ns or longer, making sure that we obtained a stable MD trajectory for each of the simulated structures. The time step used for the MD simulations was 2 fs. Periodic boundary condition was used in the NPT ensemble at $T = 298.15$ K with Berendsen temperature coupling and $P = 1$ atm with isotropic molecular-based scaling.³⁷ The SHAKE algorithm³⁸ was used to fix all covalent bonds containing hydrogen atoms. The non-bonded pair list was updated every 25 steps. The particle mesh Ewald (PME) method³⁹ was used to treat long-range electrostatic interactions. 10 Å was used as the none-bonded cutoff.

Free Energy Simulation

Free energy perturbation (FEP)^{30,40} can be performed to evaluate free energy change caused by a small structural change. The FEP method, in combination with MD simulation, has been used to study protein-ligand interaction⁴¹⁻⁴³ and protein stability.^{44,45} All of the previously reported FEP simulations on the mutation of a protein were carried out on the stable structures of the systems. In the present study, we performed the FEP simulations on the rate-determining transition state structure (*i.e.* TS1), in addition to the stable free enzyme structures, in order to predict the mutation-caused change of the catalytic efficiency for BChE-catalyzed hydrolysis of (-)-cocaine. We aimed to develop an FEP-based computational protocol which can be used to predict the catalytic efficiency change from the (-)-cocaine hydrolysis catalyzed by a BChE mutant (or wild-type) to that catalyzed by another BChE mutant.

Depicted in Figure 1 are the free energy changes associated with two reaction systems: one is the (-)-cocaine hydrolysis catalyzed by a BChE mutant (or the wild-type), denoted by Enzyme 1 or E(1); the other is the (-)-cocaine hydrolysis catalyzed by another BChE mutant, denoted by Enzyme 2 or E(2). As seen in Figure 1, the catalytic efficiency, *i.e.* $k_{\text{cat}}(i)/K_{\text{M}}(i)$, for the (-)-cocaine hydrolysis catalyzed by enzyme E(*i*) is determined by the Gibbs free energy change $\Delta G(i)$ of the reaction system from E(*i*) plus substrate S, *i.e.* (-)-cocaine, to the corresponding rate-determining transition state TS1(*i*). $\Delta G(i)$ is the sum of the enzyme-substrate binding free energy $\Delta G_{\text{ES}}(i)$ and the activation free energy $\Delta G_{\text{av}}(i)$:

$$\Delta G(i) = \Delta G_{\text{ES}}(i) + \Delta G_{\text{av}}(i), i = 1 \text{ and } 2. \quad (1)$$

Assuming that a mutation on an amino acid residue can change the enzyme from E(1) to E(2), we want to know the corresponding free energy change from $\Delta G(1)$ to $\Delta G(2)$ for the computational design of the high-activity mutants of the enzyme. There are two possible paths to determine the free energy change $\Delta\Delta G(1 \rightarrow 2) \equiv \Delta G(2) - \Delta G(1)$. One path is to directly calculate $\Delta G_{\text{ES}}(i)$ and $\Delta G_{\text{av}}(i)$ associated with E(1) and E(2), which is very computationally demanding in terms of the level of theory. For an alternative path, the relatively less-demanding FEP simulations allow us to estimate $\Delta\Delta G(1 \rightarrow 2)$ by determining the free energy changes ΔG_{E} and ΔG_{TS1} from E(1) to E(2):

$$\Delta\Delta G(1 \rightarrow 2) = \Delta G_{\text{TS1}} - \Delta G_{\text{E}} \quad (2)$$

where ΔG_{E} and ΔG_{TS1} are the free energy changes from E(1) to E(2) for the free enzyme and TS1, respectively. ΔG_{E} and ΔG_{TS1} were estimated by performing the FEP simulations in the present study. By using the calculated $\Delta\Delta G(1 \rightarrow 2)$, the ratio of the catalytic efficiency associated with E(2) to that associated with E(1) can be evaluated, *via*

$$\Delta\Delta G(1 \rightarrow 2) = -RT \ln \frac{k_{\text{cat}}(2)/K_{\text{M}}(2)}{k_{\text{cat}}(1)/K_{\text{M}}(1)}. \quad (3)$$

Equation (3) can also be used to derive the experimental $\Delta\Delta G(1 \rightarrow 2)$ value from the experimental ratio of the catalytic efficiency associated with E(2) to that associated with E(1).

We tested the above FEP-based approach for two mutations associated with A328W/Y332A \rightarrow A328W/Y332G and A328W/Y332G \rightarrow A328W/Y332G/A199S. The mutation associated with the BChE mutant change from A328W/Y332A to A328W/Y332G is the change of residue #332 from Ala to Gly, whereas the mutation associated with the BChE mutant change from A328W/Y332G to A328W/Y332G/A199S is the change of residue #199 from Ala to Ser. For technical reason, it is always more convenient to perform an FEP simulation from a larger side chain to a smaller side chain. So, for A328W/Y332G \rightarrow A328W/Y332G/A199S, we actually carried out our FEP simulation from A328W/Y332G/A199S to A328W/Y332G and used the following energy relationship:

$$\Delta\Delta G(1 \rightarrow 2) = -\Delta\Delta G(2 \rightarrow 1) \quad (4)$$

For the diminishing atoms during the perturbation simulation from a larger side chain to a smaller side chain, the dummy atoms were added to the perturbed residue to keep the number of atoms constant (see Figure 2). Thus, some normal atoms in the starting residue were gradually mutated to the dummy atoms in the perturbed residue. As seen in Figure 2, for the atom types before and after the perturbation, the dummy atoms were given a new atom type "DH" to define their new properties, in which the charges and the non-bond parameters of the dummy atoms were set to zero so that the dummy atoms did not have electrostatic and van der Waals interactions with other atoms. Furthermore, all of the bond and angle parameters involving the dummy atoms were the same as their counterparts in the initial structure in order to keep the structural skeletons unchanged. The default choice INTPRT = 0 was used to make

sure that the bonded interactions of the dummy atoms were excluded from the final calculation on the total energy of the perturbed system. The FEP simulations were carried out by using the Gibbs module of Amber7 with the “fixed width window growth” method.³⁴ The simulation process was similar to that in the aforementioned MD simulation, except that the time step was 1 fs.

To enlarge the phase space searched by the FEP calculation, for each perturbation, 10 different conformations extracted from the stable MD trajectory were used as the initial structures of the perturbation simulations. The finally calculated ΔG_{TS1} or ΔG_E value is the average of the 10 ΔG_{TS1} or ΔG_E values associated with the 10 initial structures. Each initial structure was first energy-minimized for 1,000 cycles, followed by 40 ps MD simulation for the heating and equilibration, prior to the FEP calculation. For each FEP calculation, we used 51 windows with 1,250 steps of equilibration and 1,250 steps for data collection, with both forward and backward directions. Thus, for the FEP simulation on each mutation, we performed the MD simulations for a total of $2,500 \times 51 \times 10 = 1,275,000$ steps or $1,275,000 \times 0.001 = 1.275$ ns. Some FEP simulations were also carried out for a doubled length of time in order to verify that the simulations were sufficiently long.

Results and Discussion

In order to predict the $\Delta\Delta G(1\rightarrow 2)$ value and the catalytic efficiency change for the A199S mutation associated with the change from the A328W/Y332G mutant to the A328W/Y332G/A199S mutant of BChE, the actual perturbation of our FEP simulations is the change from A328W/Y332G/A199S BChE to A328W/Y332G BChE. So, we first performed MD simulations on both the A328W/Y332G/A199S BChE and the corresponding TS1 structure in water. A stable MD trajectory was obtained for each MD simulation. As an example, the time-dependence of some key internuclear distances in the MD-simulated TS1 structure is depicted in Figure 3(A). 10 snapshots of the MD-simulated TS1 structure within the stable trajectory were used as the starting structures to perform the FEP simulations on the transition state. 10 snapshots of the MD-simulated A328W/Y332G/A199S BChE structure within the stable trajectory were used as the starting structures to perform the FEP simulations on the free enzyme. Depicted in Figure 3 are the unperturbed and perturbed structures during the FEP simulations on the TS1 structure. As seen in Figure 3, a remarkable difference between the unperturbed and perturbed TS1 structures is the hydrogen bond between the (-)-cocaine carbonyl oxygen and the hydroxyl group of the unperturbed S199 residue. Such a hydrogen bond exists only in the TS1 structure for the (-)-cocaine hydrolysis catalyzed by A328W/Y332G/A199S BChE, as the hydroxyl group disappears in the perturbed TS1 structure. Thus, the TS1 structure associated with A328W/Y332G/A199S BChE is expected to be more stable than that with A328W/Y332G BChE.

Similarly, in order to predict the $\Delta\Delta G(1\rightarrow 2)$ value and the catalytic efficiency change for the A332G mutation associated with the change from the A328W/Y332A mutant to the A328W/Y332G mutant of BChE, we performed MD simulations on both the A328W/Y332A BChE and the corresponding TS1 structure in water. For each MD-simulated structure (the free enzyme or TS1), 10 snapshots of the MD-simulated structure within the stable trajectory were used as the starting structures to perform the FEP simulations. There were no dramatic changes in terms of hydrogen bonds from the unperturbed structures (associated with A328W/Y332A BChE) to the perturbed structures (associated with A328W/Y332G BChE) during the FEP simulations on both the free enzyme and TS1.

Summarized in Table 1 are the energetic results obtained from the FEP simulations. As seen in Table 1, the $\Delta\Delta G(A328W/Y332A\rightarrow A328W/Y332G)$ and $\Delta\Delta G(A328W/Y332G\rightarrow A328W/Y332G/A199S)$ values were predicted to be -0.22 and -1.94 kcal/mol, respectively, according

to the FEP simulations. We also repeated the FEP calculations on the structural change from A328W/Y332G/A199S BChE to A328W/Y332G BChE with the double length of the simulation in each window and obtained a new $\Delta\Delta G(\text{A328W/Y332G} \rightarrow \text{A328W/Y332G/A199S})$ value of -2.02 kcal/mol. The difference between the two $\Delta\Delta G(\text{A328W/Y332G} \rightarrow \text{A328W/Y332G/A199S})$ values is smaller than 0.1 kcal/mol, suggesting that the length of the simulation is adequate. Further, a careful check of the energetic data obtained from the FEP simulations revealed that the calculated $\Delta\Delta G(\text{A328W/Y332A} \rightarrow \text{A328W/Y332G})$ value of -0.22 kcal/mol is mainly attributed to the change of the van der Waals interactions in the TS1 structure. In contrast, the calculated $\Delta\Delta G(\text{A328W/Y332G} \rightarrow \text{A328W/Y332G/A199S})$ value of -1.94 kcal/mol is mainly attributed to the formation of the additional hydrogen bond with the hydroxyl group of S199 side chain in the perturbed TS1 structure. So, the FEP calculations predict that the catalytic efficiency ($k_{\text{cat}}/K_{\text{M}}$) of A328W/Y332G BChE should be slightly higher than that of A328W/Y332A BChE and that the catalytic efficiency ($k_{\text{cat}}/K_{\text{M}}$) of A328W/Y332G/A199S BChE should be significantly higher than that of A328W/Y332G BChE against (-)-cocaine.

It is important to compare the calculated $\Delta\Delta G(\text{A328W/Y332A} \rightarrow \text{A328W/Y332G})$ and $\Delta\Delta G(\text{A328W/Y332G} \rightarrow \text{A328W/Y332G/A199S})$ values with the corresponding experimental results. The catalytic parameters of A328W/Y332A BChE against (-)-cocaine were measured to be $k_{\text{cat}} = 154 \text{ min}^{-1}$ and $K_{\text{M}} = 18 \text{ }\mu\text{M}$.²³ A328W/Y332A BChE has a ~9.4-fold improved catalytic efficiency ($k_{\text{cat}}/K_{\text{M}}$) compared to wild-type BChE against (-)-cocaine ($k_{\text{cat}} = 4.1 \text{ min}^{-1}$ and $K_{\text{M}} = 4.5 \text{ }\mu\text{M}$).²³ The catalytic efficiency ($k_{\text{cat}}/K_{\text{M}}$) of A328W/Y332G BChE was estimated to be slightly higher than $k_{\text{cat}}/K_{\text{M}}$ of A328W/Y332A BChE against (-)-cocaine in our previous work (although the specific k_{cat} and K_{M} values were not determined yet),²⁴ which is qualitatively consistent with the $\Delta\Delta G(\text{A328W/Y332A} \rightarrow \text{A328W/Y332G})$ value determined by the FEP simulations. The experimental catalytic efficiency of A328W/Y332G/A199S BChE has not been reported previously in literature. In order to know whether the catalytic efficiency of A328W/Y332G/A199S BChE is really higher than that of A328W/Y332G BChE against (-)-cocaine as predicted by the FEP simulations, we carried out wet experiments including the site-directed mutagenesis, protein expression, and the enzyme activity assays on the A328W/Y332G and A328W/Y332G/A199S mutants of human BChE. The activity assays for these two mutants were performed in comparison with A328W/Y332A BChE against (-)-cocaine. The experimental procedure is described in supporting material. The catalytic parameters determined by the wet experimental tests are summarized in Table 1. As seen in Table 1, $k_{\text{cat}} = 240 \text{ min}^{-1}$ and $K_{\text{M}} = 17 \text{ }\mu\text{M}$ for A328W/Y332G BChE against (-)-cocaine, and $k_{\text{cat}} = 389 \text{ min}^{-1}$ and $K_{\text{M}} = 5.4 \text{ }\mu\text{M}$ for A328W/Y332G/A199S BChE against (-)-cocaine. Thus, compared to wild-type BChE against (-)-cocaine, A328W/Y332G BChE has a ~15-fold improved catalytic efficiency and A328W/Y332G/A199S BChE has a ~79-fold improved catalytic efficiency.

By using the experimental catalytic parameters, Eq.(3) can be used to determine the corresponding $\Delta\Delta G(1 \rightarrow 2)$ values: $\Delta\Delta G(\text{A328W/Y332A} \rightarrow \text{A328W/Y332G}) = -0.29 \text{ kcal/mol}$ and $\Delta\Delta G(\text{A328W/Y332G} \rightarrow \text{A328W/Y332G/A199S}) = -0.98 \text{ kcal/mol}$. The experimentally-derived $\Delta\Delta G(\text{A328W/Y332A} \rightarrow \text{A328W/Y332G})$ value of -0.29 kcal/mol is in excellent agreement with the FEP-calculated $\Delta\Delta G(\text{A328W/Y332A} \rightarrow \text{A328W/Y332G})$ value of -0.22 kcal/mol. The experimentally-derived $\Delta\Delta G(\text{A328W/Y332G} \rightarrow \text{A328W/Y332G/A199S})$ value of -0.98 kcal/mol is also reasonably close to the FEP-calculated $\Delta\Delta G(\text{A328W/Y332G} \rightarrow \text{A328W/Y332G/A199S})$ value of -1.94 kcal/mol. The agreement between the computational predictions and the experimental kinetic data suggests that the FEP simulations on both the free enzyme and the corresponding rate-determining transition state may provide a promising protocol for rational design of high-activity mutants of an enzyme.

The above data demonstrate that the novel computational protocol based on the FEP simulations is not only convenient, but also reliable to directly evaluate the minor difference between two enzymes (*i.e.* the perturbed and unperturbed enzyme structures) in the catalytic activity. As well known, one can also perform appropriate quantum mechanical/molecular mechanical (QM/MM) or QM/MM-free energy calculations on two reactions catalyzed by both the two enzymes (*i.e.* the perturbed and unperturbed enzyme structures) and predict their catalytic activities with certain accuracy. The activity difference between the two enzymes can then be evaluated based on the predicted catalytic activities of the two enzymes. However, the sign of the small activity difference predicted in this way could be wrong when the actual activity difference between two enzymes is smaller than the computational error of the QM/MM or QM/MM-free energy calculations.

This is the first time FEP simulations are performed on the mutation of a transition state of an enzymatic reaction, although the FEP method has been used in combination with QM/MM calculations to calculate the free energy changes of the QM-MM interactions along the reaction pathway.^{46,47} The general computational strategy of the FEP simulation on a transition state can be used to study the effects of a mutation on the activation free energy for any enzymatic reaction. As well known, the experimental studies on mechanisms of enzymatic reactions usually include site-directed mutagenesis on some key amino acid residues so as to determine the effects of the mutations on the catalytic activity. The FEP-based transition-state simulations provide a convenient computational approach to reliably evaluate the effects that can directly be compared with the experimental data.

Conclusion

In order to reliably predict the mutation-caused shift of the free energy change from the free enzyme to the rate-determining transition state for human butyrylcholinesterase (BChE)-catalyzed hydrolysis of (-)-cocaine, we have developed and tested a novel computational protocol based on free energy perturbation (FEP) simulations on both the free enzyme and transition state structures. The calculated shift, *i.e.* $\Delta\Delta G(1\rightarrow 2)$, of such kind of free energy change determines the catalytic efficiency ($k_{\text{cat}}/K_{\text{M}}$) change caused by the simulated mutation transforming the enzyme 1 to enzyme 2. By using the FEP-based protocol, the $\Delta\Delta G(\text{A328W/Y332A}\rightarrow\text{A328W/Y332G})$ and $\Delta\Delta G(\text{A328W/Y332G}\rightarrow\text{A328W/Y332G/A199S})$ values were calculated to be -0.22 and -1.94 kcal/mol, respectively, thus predicting that the change from A328W/Y332A BChE to A328W/Y332G BChE should slightly improve the catalytic efficiency and that the change from A328W/Y332G BChE to A328W/Y332G/A199S BChE should significantly improve the catalytic efficiency of the enzyme against (-)-cocaine. The computational predictions are supported by the experimental data showing that $k_{\text{cat}}/K_{\text{M}} = 8.5 \times 10^6 \text{ min}^{-1} \text{ M}^{-1}$ for the A328W/Y332A mutant, $k_{\text{cat}}/K_{\text{M}} = 1.4 \times 10^7 \text{ min}^{-1} \text{ M}^{-1}$ for the A328W/Y332G mutant, and $k_{\text{cat}}/K_{\text{M}} = 7.2 \times 10^7 \text{ min}^{-1} \text{ M}^{-1}$ for the A328W/Y332G/A199S mutant. The agreement between the computational predictions and the experimental kinetic data suggests that the FEP simulations on both the free enzyme and the corresponding rate-determining transition state may be used to rationally design high-activity mutants of an enzyme. The general computational strategy of the FEP simulation on a transition state can be used to study the effects of a mutation on the activation free energy for any enzymatic reaction.

Supplementary Material

Refer to Web version on PubMed Central for supplementary material.

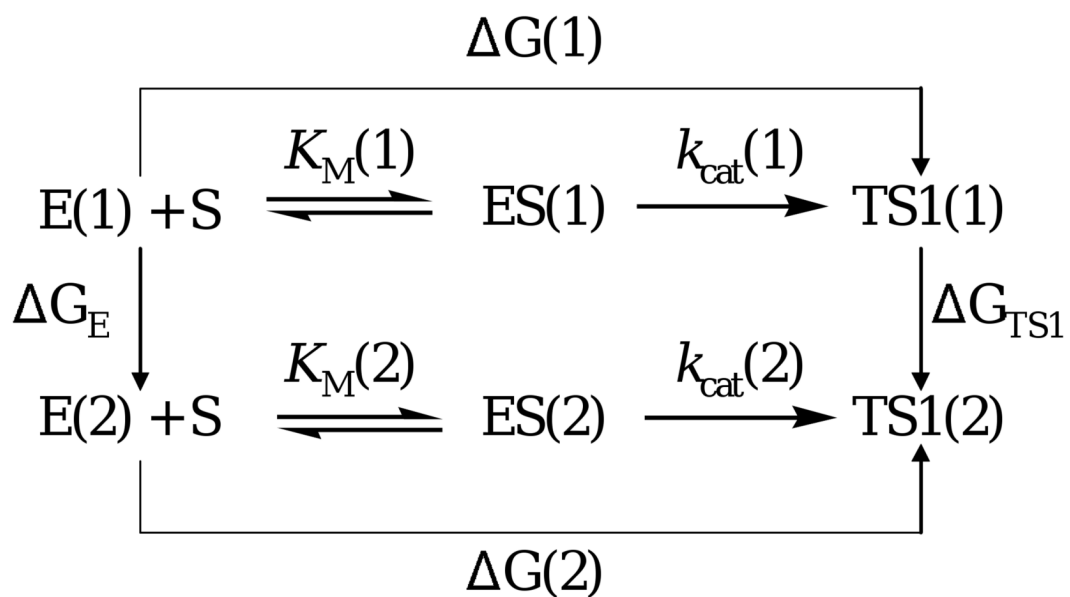
Acknowledgments

The research was supported by NIH/NIDA (grant R01 DA013930 to C.-G. Zhan). The authors also acknowledge the Center for Computational Sciences (CCS) at University of Kentucky for supercomputing time on Superdome (an HP shared-memory supercomputer, with 4 nodes for 256 processors) and on IBM X-series Cluster with 34 nodes and 1,360 processors.

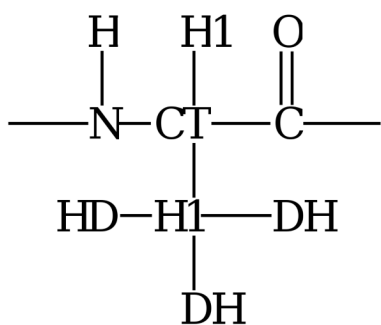
References

1. Mendelson JH, Mello NK. *N Engl J Med* 1996;334:965. [PubMed: 8596599]
2. Paula S, Tabet MR, Farr CD, Norman AB, Ball WJ Jr. *J Med Chem* 2004;47:133. [PubMed: 14695827]
3. Singh S. *Chem Rev* 2000;100:925. [PubMed: 11749256]
4. Gorelick DA. *Drug Alcohol Depend* 1997;48:159. [PubMed: 9449014]
5. Redish AD. *Science* 2004;306:1944. [PubMed: 15591205]
6. Sparenborg S, Vocci F, Zukin S. *Drug Alcohol Depend* 1997;48:149. [PubMed: 9449012]
7. Baird TJ, Deng SX, Landry DW, Winger G, Woods JH. *J Pharmacol Exp Ther* 2000;295:1127. [PubMed: 11082449]
8. Carrera MR, Ashley JA, Parsons LH, Wirsching P, Koob GF, Janda KD. *Nature* 1995;378:727. [PubMed: 7501020]
9. Carrera MR, Ashley JA, Wirsching P, Koob GF, Janda KD. *Proc Natl Acad Sci U S A* 2001;98:1988. [PubMed: 11172063]
10. Deng SX, de Prada P, Landry DW. *J Immunol Methods* 2002;269:299. [PubMed: 12379369]
11. Carrera MR, Kaufmann GF, Mee JM, Meijler MM, Koob GF, Janda KD. *Proc Natl Acad Sci U S A* 2004;101:10416. [PubMed: 15226496]
12. Dickerson TJ, Kaufmann GF, Janda KD. *Expert Opin Biol Ther* 2005;5:773. [PubMed: 15952908]
13. Gorelick DA, Gardner EL, Xi ZX. *Drugs* 2004;64:1547. [PubMed: 15233592]
14. Kantak KM. *Expert Opin Pharmacother* 2003;4:213. [PubMed: 12562311]
15. Meijler MM, Kaufmann GF, Qi L, Mee JM, Coyle AR, Moss JA, Wirsching P, Matsushita M, Janda KD. *J Am Chem Soc* 2005;127:2477. [PubMed: 15725002]
16. Zhan CG, Deng SX, Skiba JG, Hayes BA, Tschampel SM, Shields GC, Landry DW. *J Comput Chem* 2005;26:980. [PubMed: 15880781]
17. Landry DW, Zhao K, Yang GXQ, Glickman M, Georgiadis TM. *Science* 1993;259:1899. [PubMed: 8456315]
18. Kamendulis LM, Brzezinski MR, Pindel EV, Bosron WF, Dean RA. *J Pharmacol Exp Ther* 1996;279:713. [PubMed: 8930175]
19. Zhan CG, Zheng F, Landry DW. *J Am Chem Soc* 2003;125:2462. [PubMed: 12603134]
20. Lockridge O, Blong RM, Masson P, Froment MT, Millard CB, Broomfield CA. *Biochemistry* 1997;36:786. [PubMed: 9020776]
21. Gatley SJ. *Biochem Pharmacol* 1991;41:1249. [PubMed: 2009099]
22. Gatley SJ, MacGregor RR, Fowler JS, Wolf AP, Dewey SL, Schlyer DJ. *J Neurochem* 1990;54:720. [PubMed: 2299363]
23. Sun H, Pang YP, Lockridge O, Brimijoin S. *Mol Pharmacol* 2002;62:220. [PubMed: 12130672]
24. Hamza A, Cho H, Tai HH, Zhan CG. *J Phys Chem B* 2005;109:4776. [PubMed: 16851561]
25. Gao D, Cho H, Yang W, Pan Y, Yang G, Tai HH, Zhan CG. *Angew Chem Int Ed Engl* 2006;45:653. [PubMed: 16355430]
26. Pan Y, Gao D, Yang W, Cho H, Yang G, Tai HH, Zhan CG. *Proc Natl Acad Sci U S A* 2005;102:16656. [PubMed: 16275916]
27. Zhan CG, Gao D. *Biophys J* 2005;89:3863. [PubMed: 16319079]
28. Gao D, Zhan CG. *Proteins* 2006;62:99. [PubMed: 16288482]
29. Gao DQ, Zhan CG. *J Phys Chem B* 2005;109:23070. [PubMed: 16854005]
30. Kollman P. *Chem Rev* 1993;93:2395.
31. Eksterowicz JE, Houk KN. *Chem Rev* 1993;93:2439.

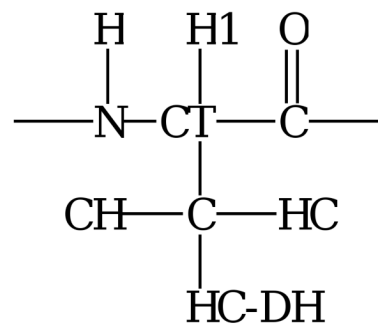
32. Nicolet Y, Lockridge O, Masson P, Fontecilla-Camps JC, Nachon F. *J Biol Chem* 2003;278:41141. [PubMed: 12869558]
33. Bernstein FC, Koetzle TF, Williams GJB, Meyer EF, Brice MD, Rodgers JR, Kennard O, Shimanouchi T, Tasumi M. *J Mol Biol* 1977;112:535. [PubMed: 875032]
34. Case, DA., et al. AMBER7. University of California; San Francisco: 2002.
35. Frisch, MJT., et al. Gaussian 03, Revision A.1. Gaussian; Pittsburgh: 2003.
36. Jorgensen WL, Chandrasekhar J, MadurAa J, Klein ML. *J Chem Phys* 1983;79:926.
37. Berendsen HJC, Postma JPM, van Gunsteren WF, DiNola A, Haak JR. *J Chem Phys* 1984;81:3684.
38. Ryckaert JP, Ciccotti G, Berendsen HJC. *J Comput Phys* 1977;23:327.
39. Essmann U, Perera L, Berkowitz ML, Darden T, Lee H, Pedersen LG. *J Chem Phys* 1995;103:8577.
40. Beveridge DL, Dicapua FM. *Annu Rev of Biophys Biophys Chem* 1989;18:431. [PubMed: 2660832]
41. Jarmula A, Cieplak P, Les A, Rode W. *J Comput Aided Mol Des* 2003;17:699. [PubMed: 15068368]
42. Udier-Blagovic M, Tirado-Rives J, Jorgensen WL. *J Med Chem* 2004;47:2389. [PubMed: 15084137]
43. Zhang W, Hou TJ, Qiao XB, Huai S, Xu XJ. *J Mol Model* 2004;10:112. [PubMed: 14986176]
44. Danciulescu C, Nick B, Wortmann FJ. *Biomacromolecules* 2004;5:2165. [PubMed: 15530030]
45. Funahashi J, Sugita Y, Kitao A, Yutani K. *Protein Eng* 2003;16:665. [PubMed: 14560052]
46. Guimaraes CR, Repasky MP, Chandrasekhar J, Tirado-Rives J, Jorgensen WL. *J Am Chem Soc* 2003;125:6892. [PubMed: 12783541]
47. Ranaghan KE, Ridder L, Szefczyk B, Sokalski WA, Hermann JC, Mulholland AJ. *Org Biomol Chem* 2004;2:968. [PubMed: 15034619]

**Figure 1.**

The relationship between different free energy changes for the reactions catalyzed by two enzymes. $E(i)$ is the free enzyme, $ES(i)$ represents the enzyme-substrate complex, and $TS1(i)$ refers to the transition state.



(A) Gly332 after perturbation



(B) Ala199 after perturbation

Figure 2.

(A) Structure and atom types of residue #332 after the perturbation associated with A328W/Y332A→A328W/Y332G; (B) structure and atom types of residue #199 after perturbation corresponding to A328W/Y332G→A328W/Y332G/A199S.

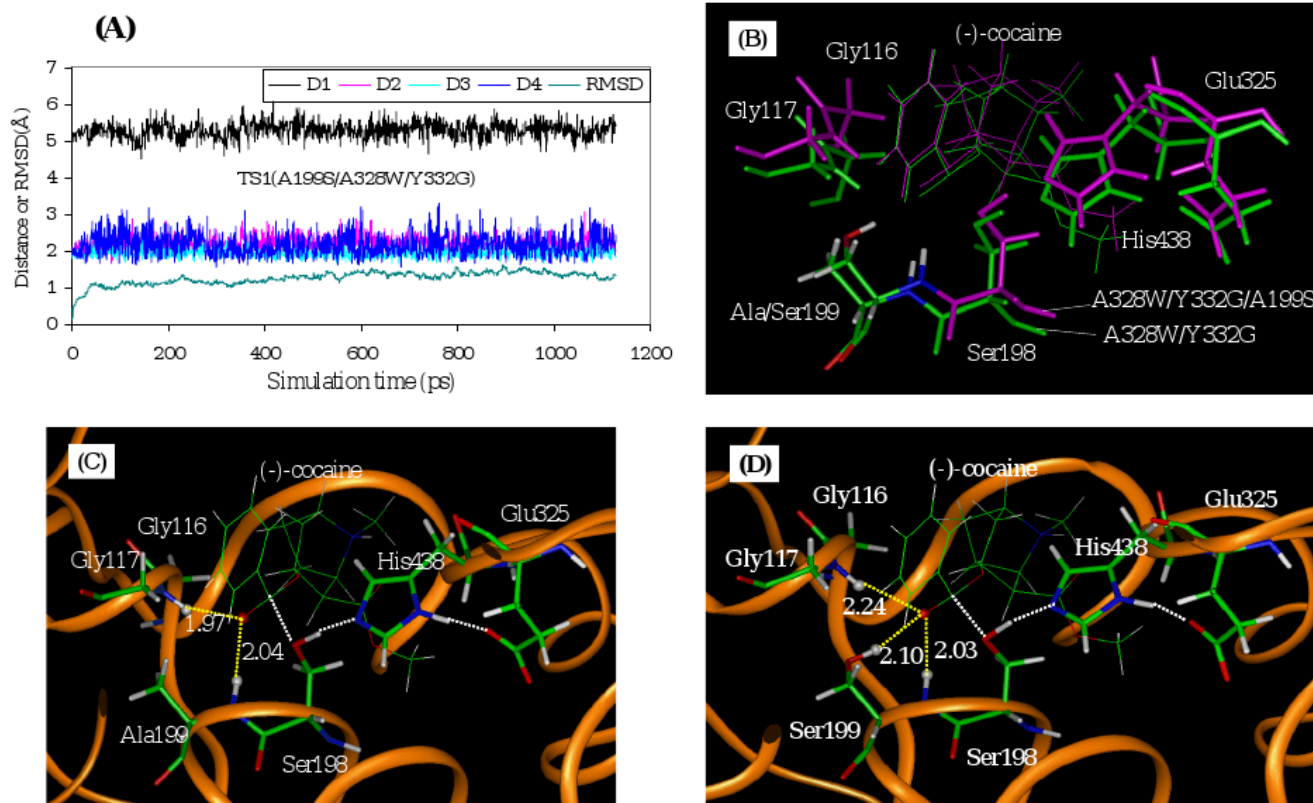
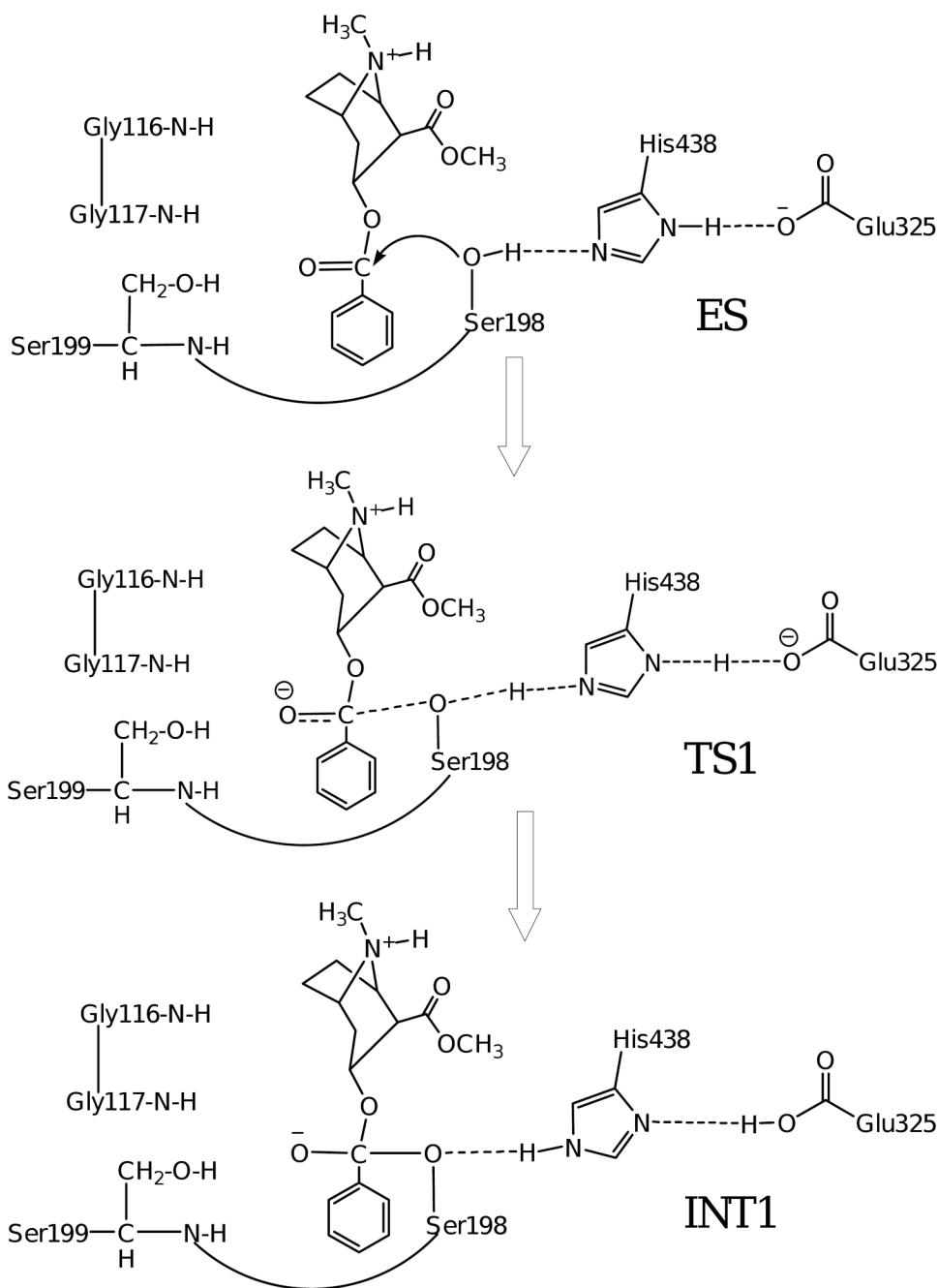


Figure 3.

(A) Plots of the key internuclear distances *versus* the time in the MD-simulated TS1 structure for (-)-cocaine hydrolysis catalyzed by A199S/A328W/Y332G BChE. Traces D1, D2, and D3 refer to the distances between the carbonyl oxygen of (-)-cocaine and the NH hydrogen of G116, G117, and S199, respectively. Trace D4 is the internuclear distance between the carbonyl oxygen of (-)-cocaine benzoyl ester and the hydroxyl hydrogen of the S199 side chain. RMSD represents the root-mean-square deviation of the simulated positions of the protein backbone atoms from those in the initial structure. (B) Superimposing of the TS1 structure corresponding to the A328W/Y332G mutant (after the perturbation, green) with that corresponding to the A328W/Y332G/A199S mutant (before the perturbation, magenta). The colors of the atoms in residue A199 (after the perturbation) or S199 (before the perturbation) are shown according to their atom types. (C) The TS1 structure with the A328W/Y332G mutant after the perturbation. The dashed lines in yellow indicate the hydrogen bonds between (-)-cocaine and the oxyanion hole of the mutant. The simulated average distances are given for the hydrogen bonds. The dashed lines in white refer to the transition bonds. The atoms highlighted as balls include several key H atoms (grey balls) from the oxyanion hole of the protein and the O atom (red ball) of the (-)-cocaine carbonyl group. (D) The TS1 structure with the A328W/Y332G/A199S mutant before the perturbation.

**Scheme 1.**

Schematic representation of the first reaction step for (-)-cocaine hydrolysis catalyzed by a BChE mutant with an A199S mutation. S199 should be A199 for the (-)-cocaine hydrolysis catalyzed by wild-type BChE and other mutants considered in this study.

Table 1

The FEP-calculated free energy changes (in kcal/mol) in comparison with the experimental kinetic data for (-)-cocaine hydrolysis catalyzed by BChE mutants.

Mutation	Calc. ^a			Expt. ^b
	ΔG_E	ΔG_{TS1}	$\Delta\Delta G(1\rightarrow2)$	$\Delta\Delta G(1\rightarrow2)$
A328W/Y332A \rightarrow A328W/Y332G	-5.11 (0.41)	-5.33 (0.29)	-0.22	-0.29
A328W/Y332G \rightarrow A328W/Y332G/A199S	-9.30 (0.44)	-11.24 (0.69)	-1.94	-0.98
Experimental kinetic parameters				
Mutant	k_{cat} (min ⁻¹)	K_M (μ M)	k_{cat}/K_M (min ⁻¹ M ⁻¹)	Relative k_{cat}/K_M ^d
Wild-type BChE ^c	4.1	4.5	9.1×10^5	1
A328W/Y332A ^c	154	18	8.5×10^6	9.4
A328W/Y332G	240	17	1.4×10^7	15
A328W/Y332G/A199S	389	5.4	7.2×10^7	79

^a ΔG_E and ΔG_{TS1} are the mutation-caused free energy changes for the free enzyme and transition state, respectively. The number in the parenthesis after the ΔG_E or ΔG_{TS1} value refers to the root-mean-square fluctuation (RMSF) of the ΔG_E or ΔG_{TS1} values calculated starting from the 10 initial structures.

^b The experimental $\Delta\Delta G(1\rightarrow2)$ values were derived from the experimental k_{cat}/K_M values.

^c The experimental data from ref.23.

^d The relative k_{cat}/K_M refers to the ratio of the catalytic efficiency of the BChE mutant to that of the wild-type.